

GPU-accelerated Gibbs Sampling

Alexander Terenin

Applied Mathematics and Statistics, University of California, Santa Cruz

aterenin@ucsc.edu

Shawfeng Dong

Astronomy and Astrophysics, University of California, Santa Cruz

shaw@ucsc.edu

David Draper

Applied Mathematics and Statistics, University of California, Santa Cruz

draper@ucsc.edu

August 15, 2016

Abstract

Gibbs sampling is a widely used Markov Chain Monte Carlo (MCMC) method for numerically approximating integrals of interest in Bayesian statistics and other mathematical sciences. Many implementations of MCMC methods do not extend easily to parallel computing environments, as their inherently sequential nature incurs a large synchronization cost. In this paper, we show how to do Gibbs sampling in a fully data-parallel manner on a graphics processing unit (GPU) for a large class of exchangeable models that admit latent variable representations. We demonstrate the scheme on a horseshoe probit regression model, and find that our implementation scales effectively to thousands of predictors and millions of data points simultaneously.

Keywords: Bayesian regression models, Big Data, graphics processing units, high-dimensional statistical modeling, Markov Chain Monte Carlo, parallel computing.

1 Introduction

The Bayesian statistical paradigm has a variety of desirable properties. It accounts for the uncertainty inherent in statistical inference, by producing a posterior distribution, which fundamentally contains more information about the variables of interest than a point estimate. It also propagates this uncertainty to predictive distributions, and thus does not overfit in a way that paradigms that produce only point estimates may do. Unfortunately, the computational methods required to produce a posterior distribution tend to be expensive. In particular, Markov Chain Monte Carlo (MCMC) [9, 11, 22] methods – the cornerstone of modern Bayesian computation – often do not scale well either with data set size or model complexity.

In this paper, we offer a novel way to implement MCMC for a large class of Bayesian models that admit exchangeable likelihoods. We do so by performing the computations on a *Graphics Processing Unit (GPU)*, a widely available parallel processor originally designed for 3D video use cases, but well suited to a variety of other tasks. In the sections that follow, we describe GPUs, characterize models in which our approach is usable, and demonstrate our method on a horseshoe probit model with $N = 1,000,000$ and $p = 1,000$. Standard computation with such N may easily take $O(\text{days})$ – our implementation runs in $O(\text{minutes})$.

2 Previous Work

There are a number of approaches for using GPUs for accelerating computation in Bayesian inference. Some approaches are completely model specific, others are generic. They include the following, in no particular order.

- *Bayesian Mixture Models*. Suchard et al. [34] review and describe GPUs, and outline a method for performing calculations needed to fit Bayesian mixture models with MCMC on a GPU.
- *Hamiltonian Monte Carlo*. Beam et al. [2] outline a method for fitting a Bayesian multinomial logistic regression model on a GPU with Hamiltonian Monte Carlo.
- *Parallel Tempering*. Mingas and Bouganis [23] describe a method for sampling from multimodal distributions with parallel tempering, using hardware acceleration in the form of a field-programmable grid array (FPGA), and compare their method with GPU implementations.
- *Sequential Monte Carlo*. Lee et al. [16] review the architecture, programming model, and performance of GPUs and describe methods for running importance-sampling-based algorithms such as Sequential Monte Carlo on GPUs.
- *State Augmented Marginal Estimation*. Seita et al. [32] proposes a way to use GPUs to accelerate an annealed variant of Gibbs sampling, used for obtaining high-quality point estimates without getting stuck in local optima in discrete state spaces.
- *Latent Dirichlet Allocation*. A number of authors have created GPU-accelerated algorithms for Latent Dirichlet Allocation. These include Yan et al. [38] (using Collapsed Gibbs sampling) and Canny and Zhao [4] (using Variational Bayes).
- *Deep Learning*. Krizhevsky [13] outlines a way to employ GPUs to accelerate algorithms used for deep learning. Though these algorithms are not Bayesian, in the computational sense of producing a distribution function as output, they are meaningful to include because the success of deep learning illustrates the sheer complexity of models that can be fitted with GPUs.

This review is brief and emphatically not exhaustive. Many other authors have created GPU-accelerated algorithms for Bayesian inference, and in a larger context, for statistical inference. However, most methods are model-specific, and further work is needed to create methods for Bayesian inference that are generic, applying to large classes of models.

3 Review and Description of GPUs

A GPU can be thought of as a massively parallel co-processor. Whereas a CPU typically has a few physical cores optimized for sequential serial processing, a modern GPU has thousands of smaller cores optimized for handling multiple tasks simultaneously. GPUs operate according to the *single-instruction-multiple-thread (SIMT)* [20] model, a special case of *single-instruction-multiple-data (SIMD)* [20]: every thread in a thread block must execute the same instructions, but with respect to a different location in memory. Multiple thread blocks execute concurrently on the same GPU. Whereas a CPU is designed to quickly perform a sequence of instructions with low latency, a GPU is designed to perform for data-parallel, high-throughput computing, and functions optimally when it has at least tens of thousands of simultaneous threads. These

differences between the CPU and GPU paradigms lead to sharply different programming models, and significant potential performance gains in applications that are able to take advantage of the parallelism a GPU offers. We now provide a brief overview of GPUs – for a more in-depth discussion, see Sanders and Kandrot [31].

GPUs have been employed in a variety of high-performance computing tasks. While originally designed for graphics, they have also been applied to general-purpose computing (GPGPU), and have been used in a variety of areas – Sanders and Kandrot [31] list use cases in physics, signal and image processing, computational fluid dynamics, medical imaging, environmental science, deep learning, and a variety of other areas.

There are two major general-purpose programming frameworks for GPUs, *CUDA* [25] and *OpenCL* [33]. CUDA is a proprietary framework for Nvidia GPUs, whereas OpenCL is an open standard framework for Nvidia and AMD GPUs, as well as multi-core CPUs, digital signal processors (DSPs), field-programmable gate arrays (FPGAs) and other processors or hardware accelerators. The frameworks are similar in principle, but scientific computing at present generally focuses on CUDA, because it has a larger user base and better availability of software libraries for primitive tasks such as matrix operations and random number generation. We focus here on Nvidia GPUs and describe them in Nvidia-specific terminology – the structure and terminology for AMD GPUs is largely analogous.

A GPU is organized hierarchically in both hardware and software. The smallest unit that performs computations is a *thread processor* (or *core*). Each thread has access to its index, and typically uses it to find its unique data point to perform operations on. Thread processors are grouped together into *streaming multiprocessors*, which execute code organized into *thread blocks*. A thread block executes groups of 32 threads called *warps* in parallel. Each streaming multiprocessor contains *shared memory* that may be accessed by different warps inside the corresponding thread block. The GPU itself is composed of multiple streaming multiprocessors, which have access to *global memory*. A function in CUDA that runs directly on the GPU is called a *kernel*, and is launched with respect to a *grid* of thread blocks.

This architecture has a number of implications for performance. Each thread in a warp must perform the same instruction at every point in time. This means that within a warp, if an *if/else* statement is encountered, the threads will first execute the *if* portion, *wait until it completes*, and then execute the *else* portion. This is referred to as *warp divergence*, and should be minimized to maintain good performance. Global memory is much slower than other types of memory, and should be accessed sparingly – ideally, only to obtain data at the beginning of a computation and to output the results of the computation at the end. As noted above, due to both the large number of parallel threads and relatively high latency – which can be hidden by scheduling multiple computations – a GPU should perform at least tens of thousands of tasks in parallel to be effectively utilized.

Thus, for optimal performance, the computation of interest should permit a high degree of parallelism. Threads should execute code with as few *if/else* statements that evaluate to multiple values within one warp as possible. They should also rely on computations performed by other threads as little as possible, and only by utilizing shared memory within their respective thread block. We demonstrate below that the class of Gibbs samplers we consider effectively meets all of these requirements.

The CUDA Toolkit includes a number of GPU-accelerated libraries. We use *cuBLAS* (a GPU-accelerated library for performing matrix operations), *cuRAND* (for parallel random number generation), and *cuSOLVER* (for solving linear systems) [26]. Our implementation is written in Scala [28], a general-purpose compiled language similar to and interoperable with Java [10]. We interface with CUDA using *JCuda* [12], a set of

Java bindings for CUDA, to call GPU code. Custom CUDA kernels are written in CUDA C [26].

4 Exchangeable Models

As noted above, to run efficiently on a GPU an algorithm must demonstrate a large amount of parallelism, with minimal interaction between its parts. We now show that data-augmentation-based Gibbs samplers arising from Bayesian statistical models with *exchangeable* likelihoods possess sufficient parallelism.

Let

$$f(\mathbf{y} \mid \boldsymbol{\theta}) = \prod_{i=1}^N f(y_i \mid \boldsymbol{\theta}) \quad (1)$$

be an exchangeable likelihood arising from an application of De Finetti’s Theorem [8], and let $\pi(\boldsymbol{\theta})$ be the prior for $\boldsymbol{\theta}$. Suppose that for each y_i there exists a z_i such that

$$f(y_i \mid \boldsymbol{\theta}) = f(y_i \mid z_i)f(z_i \mid \boldsymbol{\theta}), \quad (2)$$

yielding the data-augmented exchangeable likelihood

$$f(\mathbf{y} \mid \boldsymbol{\theta}) = \prod_{i=1}^N f(y_i \mid \boldsymbol{\theta}) = \prod_{i=1}^N f(y_i \mid z_i)f(z_i \mid \boldsymbol{\theta}). \quad (3)$$

Such likelihoods arise in a large class of models. In fact, complex hierarchical Bayesian models are often built by starting with a set of exchangeability assumptions about the data, and specifying a generative process that yields a likelihood expressed in terms of latent variables as above by construction. Now consider the posterior distribution

$$f(\boldsymbol{\theta} \mid \mathbf{y}) \propto f(\mathbf{y} \mid \boldsymbol{\theta})\pi(\boldsymbol{\theta}) = \left[\prod_{i=1}^N f(y_i \mid \boldsymbol{\theta}) \right] \pi(\boldsymbol{\theta}) = \left[\prod_{i=1}^N f(y_i \mid z_i)f(z_i \mid \boldsymbol{\theta}) \right] \pi(\boldsymbol{\theta}). \quad (4)$$

The full conditional distributions for

$$f(z_i \mid y_i, \boldsymbol{\theta}) \propto f(y_i \mid z_i)f(z_i \mid \boldsymbol{\theta}) \quad (5)$$

with $i = 1, \dots, N$, and

$$f(\boldsymbol{\theta} \mid \mathbf{z}) \propto \left[\prod_{i=1}^N f(z_i \mid \boldsymbol{\theta}) \right] \pi(\boldsymbol{\theta}) \quad (6)$$

can be used to construct a suitable MCMC algorithm. Often, these full conditional distributions can be recognized from known families of distributions and used to construct a *Gibbs sampler* [9]. In what follows, “ $\mid -$ ” stands for “given all other components of the model.”

Algorithm 1.

- (a) Initialize arbitrary $(\boldsymbol{\theta}^0, \mathbf{z}^0)$.
- (b) For $k = 1$ to $k = N_{\text{MC}}$:
 - (i) Sample $\boldsymbol{\theta}^k \mid -$.

- (ii) Sample $z_1^k \mid -$.
- (iii) ...
- (iv) Sample $z_N^k \mid -$.

Where this is not possible, Metropolis-Hastings [22] steps can instead be performed, yielding a *Metropolis-within-Gibbs* sampler. Both algorithms will in the limit yield samples from the posterior distribution $f(\boldsymbol{\theta}, \mathbf{z} \mid \mathbf{y})$, which yields the target distribution $f(\boldsymbol{\theta} \mid \mathbf{y})$ marginally.

Now, suppose that N is large. On a CPU, these algorithms will be slow: there are N full conditionals that each need to be updated at every step of the algorithm. However, notice that $f(\boldsymbol{\theta} \mid \mathbf{z})$ does not depend on the data, and that

$$z_i \mid y_i, \boldsymbol{\theta} \perp\!\!\!\perp z_{-i} \mid y_i, \boldsymbol{\theta} \quad (7)$$

for all i (in which z_{-i} means all of the z values except z_i), i.e. all of the variables z_i are full-conditionally independent. Hence, they can be sampled all at once in parallel on a GPU. This observation forms the basis of our method.

Algorithm 2.

- (a) Initialize arbitrary $(\boldsymbol{\theta}^0, \mathbf{z}^0)$.
- (b) For $k = 1$ to $k = N_{\text{MC}}$:
 - (i) Sample $\boldsymbol{\theta}^k \mid -$.
 - (ii) Sample $z_1^k \mid -$, ..., $z_N^k \mid -$ simultaneously in parallel.

Algorithm 2 is a standard MCMC algorithm, so no additional convergence theory for it is needed for it to be valid. Our conditional independence observation is not new – indeed, it is rather obvious and has been known for decades. However, recent advances in GPU programming, such as implementation and wide availability of linear solvers needed for models that include matrix inversion, have made running GPU-accelerated Gibbs sampling tractable. We focus our attention in what follows on implementation and performance.

5 Example: Horseshoe Probit Regression

We illustrate GPU-accelerated Gibbs sampling with the horseshoe probit regression model [1, 5], which has a likelihood function specified (for $i = 1, \dots, N$) by

$$y_i \mid z_i = \text{round}[\Phi(z_i)] \quad z_i \mid \mathbf{X}_i, \boldsymbol{\beta} \sim \text{N}(\mathbf{X}_i \boldsymbol{\beta}, 1) \quad (8)$$

and the following prior:

$$\beta_i \mid \lambda_i, \tau \sim \text{N}(0, \lambda_i^2 \tau^2) \quad \lambda_i \sim \text{C}^+(0, 1) \quad \tau \sim \text{C}^+(0, 1). \quad (9)$$

Here $\text{C}^+(0, 1)$ is a standard Cauchy distribution truncated to \mathbb{R}^+ and \mathbf{X}_i and $\boldsymbol{\beta}$ are $(1 \times p)$ and $(p \times 1)$ vectors of data and regression parameters, respectively. We base our algorithm on the Gibbs sampler for

probit regression in Albert and Chib [1], combining it with the hierarchical representation of the horseshoe and corresponding Gibbs steps in Makalic and Schmidt [17]. By recognizing that

$$\kappa \sim \text{IG}(1, \theta) \implies \kappa^{-1} \sim \text{G}(1, \theta) = \text{Exp}(\theta), \quad (10)$$

we arrive at the following full conditionals, suppressing the conditioning bar | henceforth for readability:

$$z_i \sim \text{TN}(\mathbf{x}_i \boldsymbol{\beta}, 1, y_i) \quad \lambda_j^{-2} \sim \text{Exp} \left[\nu_j^{-1} + \frac{\tau^{-2} \beta_j^2}{2} \right] \quad \nu_j^{-1} \sim \text{Exp}(1 + \lambda_j^{-2}) \quad (11)$$

$$\boldsymbol{\beta} \sim \text{N}(\boldsymbol{\Sigma} \mathbf{X}^T \mathbf{z}, \boldsymbol{\Sigma}) \quad \tau^{-2} \sim \text{IG} \left[\frac{p+1}{2}, \xi^{-1} + \frac{1}{2} \sum_{j=1}^p \lambda_j^{-2} \beta_j^2 \right] \quad \xi^{-1} \sim \text{Exp}(1 + \tau^{-2}), \quad (12)$$

where $\boldsymbol{\Sigma} = (\mathbf{X}^T \mathbf{X} + \tau^{-2} \boldsymbol{\Lambda}^{-2})^{-1}$, $\boldsymbol{\Lambda}^{-2} = \text{diag}(\lambda_1^{-2}, \dots, \lambda_p^{-2})$, and $\text{TN}(\mu, \sigma^2, y_i)$ is a truncated normal with location μ and squared scale σ^2 , truncated to \mathbb{R}^+ if $y_i = 1$ and \mathbb{R}^- if $y_i = 0$.

Our algorithm performs the following updates:

- (i) Sample \mathbf{z} , and $\boldsymbol{\lambda}^{-2}$ followed by τ^{-2} in parallel.
- (ii) Sample $\boldsymbol{\beta}$, $\boldsymbol{\nu}^{-1}$, and ξ^{-1} in parallel.

We now describe the large degree of parallelism exploited by this sampler, and show that every calculation here is well-suited to a GPU, in the sense that everything can be performed in parallel with minimal warp divergence.

$\boldsymbol{\beta}$:

- i. Precompute $\mathbf{X}^T \mathbf{X}$ before starting the algorithm using *cublasSgemm*.
- ii. Calculate $\boldsymbol{\Sigma}^{-1} = \mathbf{X}^T \mathbf{X} + \tau^{-2} \boldsymbol{\Lambda}^{-2}$ using *cublasSaxpy*.
- iii. Perform a Cholesky decomposition to find $\mathbf{R}^{-1} = \text{Chol}(\boldsymbol{\Sigma}^{-1})$ using *cusolverDnSpotrf*.
- iv. Draw \mathbf{s} , a vector of IID standard normals using *curandGenerateNormal*.
- v. Compute $\mathbf{R}\mathbf{s}$ by solving the triangular system $\mathbf{R}^{-1}\mathbf{v} = \mathbf{s}$ for \mathbf{v} using *cublasStrsv*.
- vi. Compute $\mathbf{X}^T \mathbf{z}$ using *cublasSgemv*.
- vii. Compute $\boldsymbol{\mu} = \boldsymbol{\Sigma} \mathbf{X}^T \mathbf{z}$ by solving the linear system $\boldsymbol{\Sigma}^{-1} \boldsymbol{\mu} = \mathbf{X}^T \mathbf{z}$ for $\boldsymbol{\mu}$, in process reusing the already-computed Cholesky decomposition, using *cusolverDnSpotrs*.
- viii. Compute $\boldsymbol{\beta} = \mathbf{R}\mathbf{s} + \boldsymbol{\mu}$ using *cublasSaxpy*.

\mathbf{z} :

- i. Calculate $\boldsymbol{\mu} = \mathbf{X}\boldsymbol{\beta}$ using *cublasSgemv*.
- ii. Draw \mathbf{z} by using the following sampling routine, implemented as a custom CUDA kernel.
 - a. Compute $y_i^* = 2y_i - 1$ and $\mu_i^* = \mu_i y_i^*$. Note that if $y_i = 1$ then $y_i^* = 1$, and if $y_i = 0$ then $y_i^* = -1$.
 - b. If $\mu^* > 0.47$, use a Gaussian rejection sampler.
 - i. Draw $s_i \sim \text{N}(0, 1)$ and compute $z_i^{\text{prop}} = s_i + \mu_i^*$.

- ii. Return $z_i = y_i^* z_i^{\text{prop}}$ if $z_i^{\text{prop}} > 0$. Otherwise, draw a new Gaussian and try again.
- c. Else, use the Exponential rejection sampler described in Robert [29].
 - i. Calculate proposal parameter θ_i in [29]. The formula for θ_i is modified for non-zero mean and truncation to \mathbb{R}^+ , and acceptance probability ρ_i is modified accordingly as well.
 - ii. Draw $u_i^{(1)} \sim U(0, 1)$ and $u_i^{(2)} \sim U(0, 1)$, compute $z_i^{\text{prop}} = -\theta_i^{-1} \ln(u_i^{(1)}) \sim \text{Exp}(\theta_i)$, and ρ_i .
 - iii. Return $z_i = y_i^* z_i^{\text{prop}}$ if $u_i^{(2)} < \rho_i$. Otherwise, draw two new uniforms and try again.
- d. Note that there are three possible kinds of warp divergence in this routine that need to be minimized. The first kind arises because the two rejection samplers cannot be performed in parallel – this is unavoidable unless all threads in a warp have $\mu^* < 0.47$ or vice versa. The second kind arises from the iterative nature of rejection sampling: a warp will finish only when *all* threads have accepted – this is kept under control because both samplers are efficient, with an overall worst-case acceptance probability of around 2/3 for μ^* in a neighborhood around 0.47, and probability near 1 everywhere else. The third kind arises because some z_i will be truncated to \mathbb{R}^+ while others are truncated to \mathbb{R}^- – this is eliminated completely by introducing y_i^* .

$\lambda^{-2}, \nu^{-1}, \xi$:

- i. Draw \mathbf{u} , a vector of IID uniforms, using *curandGenerateUniform*.
- ii. Calculate parameter $\boldsymbol{\theta}$ and transform \mathbf{u} to $\text{Exp}(\boldsymbol{\theta})$ via the inversion formula $-\boldsymbol{\theta}^{-1} \ln(\mathbf{u})$, implemented as a custom CUDA kernel.

τ^{-2} :

- i. Calculate β^2 using a custom CUDA kernel.
- ii. Calculate the sum in the scale parameter by expressing it as the dot product $\lambda^{-2} \cdot \beta^2$ using *cublasSdot*.
- iii. Draw $\tau^{-2} \sim G(a, b)$ using the rejection sampler in Cheng [6], implemented as a custom CUDA kernel. This kernel involves cooperation among threads, and is described as follows.
 - a. Each of the 32 threads draws two uniforms, performs an accept-reject step independently, and writes its results to shared memory within the block, after which all threads synchronize.
 - b. Thread 1 sequentially looks through shared memory and returns once it finds an accepted value.
 - c. If all threads rejected, new proposals are computed. This is exceedingly rare for k large: each thread accepts with probability approximately 0.88 [6], so the combined acceptance probability for the entire kernel is about $1 - 3.4 \times 10^{-30}$.

Our current implementation is well-optimized in some ways and suboptimal in others. The update for β given the precision matrix avoids matrix inversion in favor of solving a linear system and a triangular system via a single Cholesky decomposition. This works because $\Sigma = \mathbf{R}^T \mathbf{R} \implies \Sigma^{-1} = \mathbf{R}^{-1} (\mathbf{R}^{-1})^T$. This is far more efficient than the following process, which we call the naive implementation because it matches up well with mathematical formulas but is a poor choice for performance.

- (1) Calculate and store $(\mathbf{X}^T \mathbf{X} + \Sigma_0)^{-1}$ by behind-the-scenes performing an LU decomposition.
- (2) Calculate $(\mathbf{X}^T \mathbf{X} + \Sigma_0)^{-1} \mathbf{X}^T \mathbf{z}$.

- (3) Use the R function *mvnorm* in the package *MASS* [37] to sample from a Multivariate Gaussian by behind-the-scenes performing an eigenvalue-eigenvector decomposition of $(\mathbf{X}^T\mathbf{X} + \Sigma_0)^{-1}$.

In addition to extra matrix decompositions which degrade performance and numerical stability, the naive implementation also calculates and stores a matrix inverse, which in general should never be done when that matrix inverse will subsequently be multiplied by another matrix or vector, as solving a linear system is mathematically equivalent and computationally cheaper. Our routine performs better, though we suspect even more efficient implementations are possible.

Most of the steps in the above routines parallelize immediately – the cuBLAS, cuRAND, and cuSOLVER library calls are highly optimized to the GPU. Our custom CUDA kernels, on the other hand, are not. The update for \mathbf{z} could be done more efficiently by, once after burn-in, sorting the data according to mean vector $\mathbf{X}\boldsymbol{\beta}$, which would minimize warp divergence as it would ensure that most warps perform the same kind of rejection sampler. Due to the additional code required to track the order of the sorted data on the GPU, we did not pursue this route.

The update for τ^{-2} could be made more efficient through the use of atomic operations or shuffle instructions in the final step. We did not pursue these because τ^{-2} is updated in parallel with \mathbf{z} , and its computational burden is comparatively tiny with little impact on performance. We note, however, that computing τ^{-2} would likely not be faster if executed by fewer than 32 threads, as the GPU would need to use a 32-thread warp to run the CUDA kernel even if some threads are doing nothing.

Our implementation mixed the cuRAND *host API* which generates fixed-size arrays of random numbers in parallel, and the cuRAND *device API*, which allows each thread to generate its own random numbers. We used the host API as much as we could, because it is far easier to implement and manage. The device API requires management of random number generator seeds and offsets on a per-thread basis. Our code works as follows.

- (1) Copy the random number generator state from global memory to local memory.
- (2) For each thread with index i , Skip forward k_i iterations in the random number generator, where k_i is chosen to ensure random numbers generated by different threads do not overlap.
- (3) Generate random numbers.
- (4) Once the computation is complete, write the last thread’s random number generator state back to global memory.

To be efficient, this requires a random number generator capable of skipping ahead k iterations in constant time for arbitrarily large k without causing warp divergence. The cuRAND default *XORWOW* random number generator [19] does not have constant-time skip ahead, and neither does the parallel version of the popular *Mersenne Twister* [21], but Salmon et al.’s counter-based *Philox* random number generator [30] does. We highly recommend *Philox* for its parallel efficiency, and because it is *Crush-resistant* (i.e. it passes all of the tests in *TestU01* [15], a suite for testing quality of random number generators) – see Manssen et al. [18] for a review of parallel random number generators.

To further accelerate the algorithm, we overlap computation and data transfer (IO) steps. For example, once $\boldsymbol{\beta}$ has been successfully updated, Monte Carlo output is downloaded off of the GPU at the same time as updates for other variables are computed. This is done by utilizing CUDA *streams*, a programmatic concept in CUDA that allows multiple kernels and memory operations to execute simultaneously in parallel.

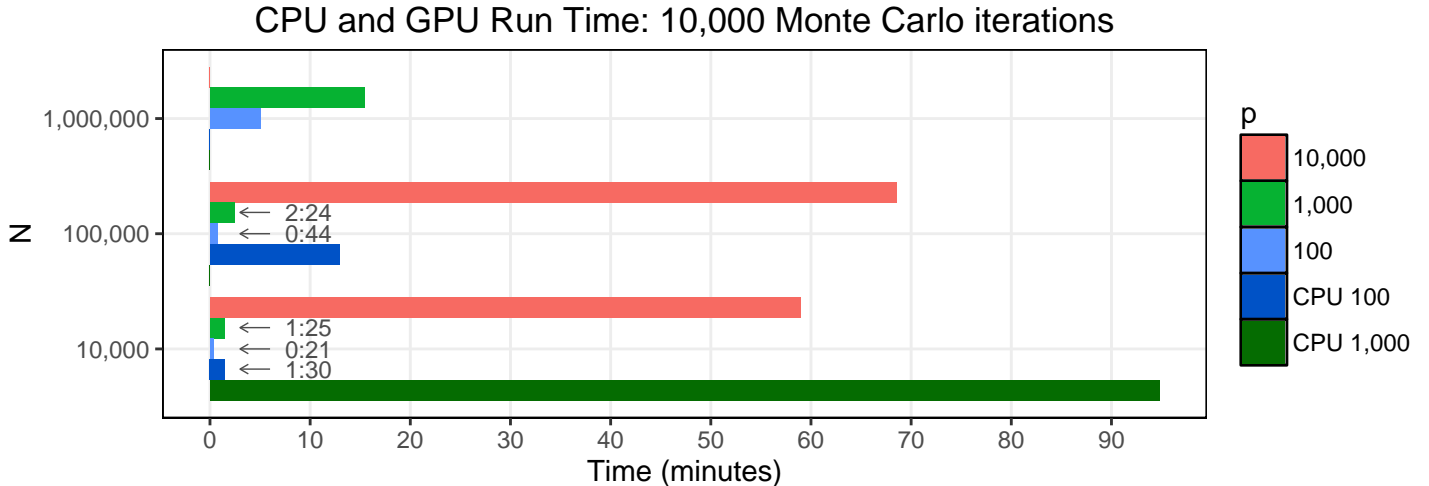


Figure 1: Comparison of GPU and CPU run time for 10,000 iterations of the horseshoe probit Gibbs sampler with synthetic data.

We ran our algorithm on the same model with multiple data sets, varying (N, p) . Performance is summarized in the following section.

6 Performance Results

6.1 Synthetic Data

We first ran our algorithm on a synthetic data set with known correct answer, generated by taking

$$x_{ij} \sim N(0, 1) \quad \beta = (1.3, 4, -1, 1.6, 5, -2, \mathbf{0}_{p-6})^T \quad \mathbf{y} \sim \text{Ber} [\Phi(\mathbf{X}\beta)] . \quad (13)$$

Our goal was to study the GPU implementation on a non-trivial model – see Chopin and Ridgway [7] for a recent discussion on the use of binary regression models for comparing performance of Bayesian algorithms.

The GPU used was a Nvidia Tesla K20m [27] with about 5GB RAM and single-precision floating-point performance of about 3.5TFLOPs, located on a node of the *Hyades* supercomputer at the Department of Astronomy and Astrophysics at the University of California, Santa Cruz. It was selected primarily for convenience: we could just as easily have used a much less expensive consumer-level GeForce card with little or no difference.

First, to compare CPU and GPU run times, we ran the algorithm with CPU-tractable values of N up to 1,000 and p up to 100. The algorithm was implemented in R in a single-threaded manner, with the same precision-matrix-based sampling scheme for β , and likewise for all other variables. The CPU used was an Intel Core i5 3210M [24] running at 2.5GHz. This is not a fast CPU by contemporary standards, but is similar to what many R users might have on their laptops, providing a meaningful rough comparison.

Then, to study scaling, we selected a variety of different combinations (N, p) with N up to 1,000,000 and p up to 10,000. Due to memory limitations, we did not run $N = 1,000,000$ and $p = 10,000$ simultaneously.

Larger data sets are possible but more difficult to accommodate because such data sets would require either multiple GPUs or streaming implementations, and we chose not to explore that possibility here – see Section 7.

We ran the Gibbs sampler for 10,000 iterations in all cases, starting from $\mathbf{z}, \boldsymbol{\beta}$ set to 0 and $\boldsymbol{\lambda}, \boldsymbol{\nu}, \tau, \xi$ set to 1. The horseshoe posterior correctly identified all non-zero values in $\boldsymbol{\beta}$ and shrank irrelevant coefficients to zero. Mixing leaves much to be desired for large N and p , but is data-dependent, so we focus on mixing in the context of real data – see Section 6.2.

Run time can be seen in figure 6.1, which shows how different values of N and p affect GPU run time, along with single-threaded CPU run time in R for comparison purposes. All times referred to in this paper are clock time.

The GPU is clearly multiple orders of magnitude faster than the CPU for all data sizes we examined – for instance, with $(N, p) = (10,000, 1,000)$, the CPU and GPU calculations took 85 minutes and 1.5 minutes, respectively. Furthermore, a 10-fold increase in data set size does not necessarily result in a 10-fold increase in run time. This is because larger data set sizes expose a larger degree of parallelism that the GPU is able to take advantage of. This is most evident for $N = 10,000$: going to $N = 100,000$ – a 10-fold increase in data set size – increases run time by a factor ranging from 1.2 to 2.1. The GPU is even faster when the data size and dimensionality are increased 10-fold simultaneously: going from $(N, p) = (10,000, 1,000)$ on CPU to $(100,000, 10,000)$ on GPU reduces run time by a factor of 1.4.

6.2 Real Data

Gastrointestinal bleeding (GI bleed) is a potentially serious health condition involving blood loss at one or more points in the gastrointestinal tract. Upper GI bleed (occurring anywhere from the mouth to the first part of the small intestine) accounts for about 20,000 deaths in the U.S. annually, and the incidence of acute upper GI hemorrhage is about 100 per 100,000 people per year. One of us (DD) was recently involved in a study in which the goal was to predict, at time t for patients hospitalized in a general medical ward with GI bleed, whether or not such patients would have an unplanned transfer to the intensive care unit (an adverse outcome to be avoided if possible) in a 4-hour time window starting at time $(t + 8)$ hours. We created a data set with $N = 372,295$ one-hour hospitalization episodes that were rendered conditionally exchangeable by a rich set of 211 clinical predictor variables. At the one-hour episode level the adverse outcome was rare (our dichotomous outcome variable had a mean of 0.0076) but highly relevant to the appropriate care path, so accurate prediction is clinically crucial.

Preliminary descriptive analysis narrowed the available independent variables down to a set of $p = 87$ interesting predictors – where *interesting* was determined according to signal-to-noise ratios in maximum-likelihood estimation – and we then used our algorithm to fit a horseshoe probit model to the resulting data set, to see how many of the interesting predictors survived the regularization process imposed by the horseshoe prior.

From a cold start, in which the \mathbf{z} and $\boldsymbol{\beta}$ were all initialized to 0 and $\boldsymbol{\lambda}, \boldsymbol{\nu}, \tau, \xi$ were started at 1, our GPU algorithm produced 10,000 iterations – 2,500 for burn-in and 7,500 for monitoring – in 1.97 minutes. All of the components of the $\boldsymbol{\beta}$ vector reached equilibrium from the cold start in about 100–200 iterations. Their mixing was slow (a typical β_i had an output trace that behaved like an $AR_1(\rho)$ time series with first-order autocorrelation $0.93 < \rho < 0.98$). Trace plots can be seen in Figure 2.

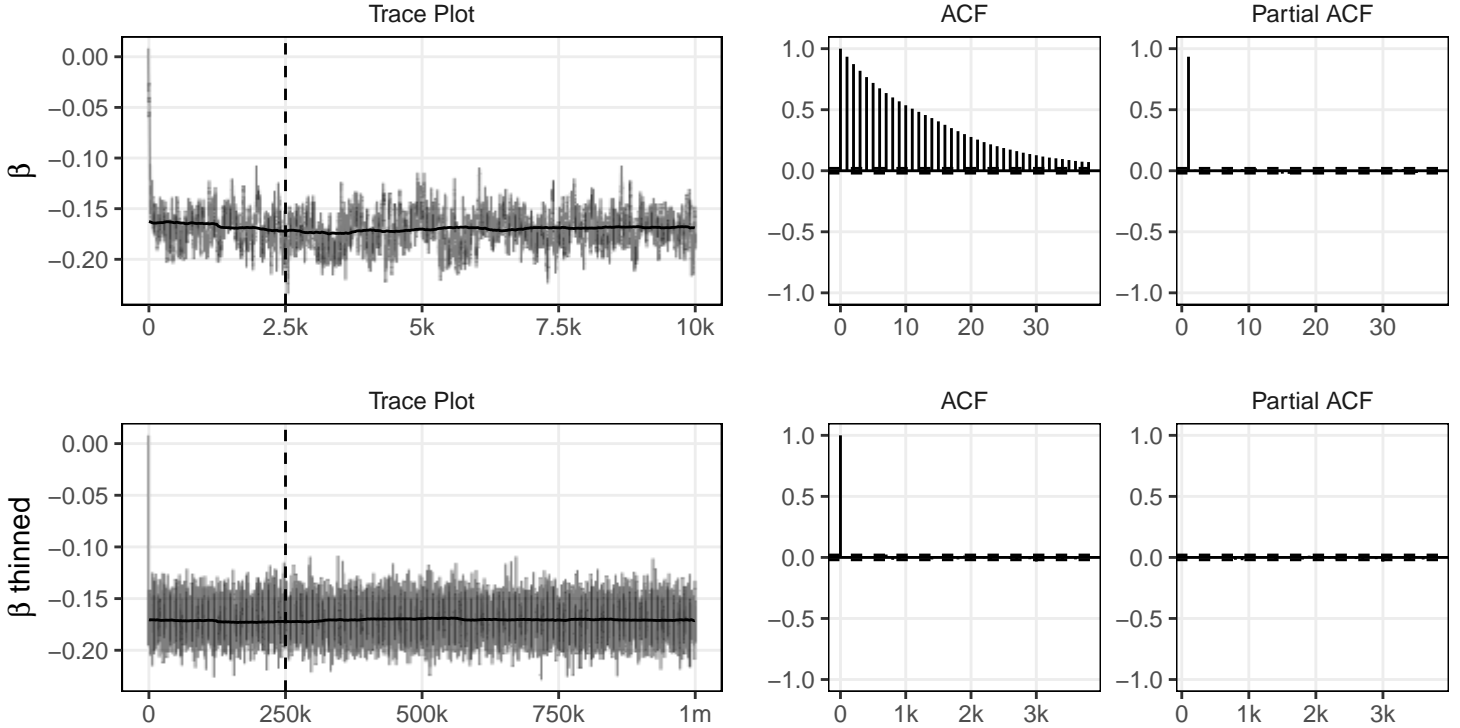


Figure 2: *Diagnostics for β_1 in the real data example of Section 6.2. Top row: original iterations, 10,000 samples. Bottom row: thinned iterations, 1,000,000 samples.*

To overcome slow mixing, we decided to run the algorithm for 1,000,000 iterations, with thinning, storing every 100th iteration in Monte Carlo output. The algorithm completed in 3 hours and 15 minutes. Trace plots can be seen in Figure 2, indicating that slow mixing is readily overcome simply by making a longer monitoring run.

The horseshoe prior shrunk about 15% of the initially-interesting predictor coefficients sharply back toward 0, leading to a more parsimonious model with a modest improvement in predictive performance.

7 Discussion

Even though MCMC methods such as Gibbs sampling are inherently sequential, our results demonstrate that the steps needed at each iteration can be sufficiently parallelizable that Gibbs sampling may be made to run orders of magnitude faster on a GPU than a CPU. We have found this to be true for our model, and we expect it to be true for other models. Exchangeable models look particularly promising, because they yield full-conditionally-independent latent variables, which can immediately be updated as a block on a GPU. Many non-exchangeable models, such as Gaussian Processes and Dirichlet Process Mixtures, can likely also benefit from GPU acceleration, if there exists a sufficient degree of available parallelism in the Gibbs steps. In our implementation, updating β is significantly faster on a GPU, in spite of the fact that $\beta_i \not\perp \beta_j$ for all $i \neq j$.

The larger versions of our synthetic data sets were large enough to take up most of the GPU’s memory,

so $(N, p) = (1,000,000, 1,000)$ was the biggest problem size we explored. There are several approaches to computing with data sets that are too big to fit in a GPU’s memory. Multiple GPUs can be used: this will introduce some performance penalty due to synchronization requirements, but may work quite well in problems that are largely limited by computationally intensive data-parallel steps. Bigger data sets may also be analyzed by using clusters of GPUs with Asynchronous Gibbs sampling – see Terenin et al. [35]. Alternatively, data can be streamed through the GPU as it is needed, rather than loaded into memory before beginning the computation. This approach has been used for point estimation in large-scale models in software packages such as *Vowpal Wabbit* [14] on CPUs and *Bidmach* [4] on GPUs, and we conjecture that it will also work well for Gibbs sampling.

The Nvidia Tesla GPU that we employed is a high-end GPU designed for scientific computing use cases. However, MCMC methods are just as well-suited to much less expensive consumer-level GeForce cards, because they are robust to numerical precision and can successfully run in floating point – see Breyer et al. [3] and Mingas and Bouganis [23]. We conjecture that using a contemporary consumer-level GPU card would have led to results similar to those presented here or perhaps better, because the Tesla K20m was released in January 2013 and newer GPUs are likely to be significantly faster.

GPUs are becoming increasingly accessible. At the time of writing, servers with scientific-computing-grade GPUs can be rented, from a variety of cloud computing providers, for less than 1 U.S. dollar per hour. Furthermore, the recent Thunderbolt 3 standard provides a specification for external GPU cases – it will soon be possible to buy a desktop grade GPU and connect it to a laptop computer using a simple cable.

Software is currently the most significant barrier to widespread adoption of GPU acceleration for Bayesian inference. The functions provided by CUDA libraries are low-level, and present a high degree of difficulty to those not already familiar with high-performance computing libraries such as BLAS and LAPACK. New frameworks are needed to bring modern programmatic concepts into the GPU software stack. These would parallel recent advances in programmatic frameworks for compute clusters, such as *Akka* [36] and *Apache Spark* [39], which made computation in the cluster environment much more user friendly through the implementation of modern concepts such as actor models, functional programming, and lazy evaluation. Similar work is needed in simplifying GPU debugging. We hope that in a few years it will be just as easy to write a Gibbs sampler on a GPU as it currently is on a CPU in a high-level language such as *R*.

Another difficulty in CUDA is lack of random number generation routines for less-common distributions. In the horseshoe probit model, we needed to implement custom CUDA kernels for sampling Exponential, Gamma, and Truncated Normal random variables. We also needed to implement a CUDA kernel for squaring arrays of numbers – while trivial to implement, this resulted in yet another file that needed to be written, debugged, and compiled before we could run our algorithm. These issues are even more pronounced in OpenCL, where there are no widely available libraries for many matrix and vector routines. We hope that future work will remove these difficulties.

Though our initial results on the horseshoe probit regression model are promising, further work is needed to study Bayesian computation on GPUs. Many algorithms beyond Gibbs sampling can likely take advantage of GPUs, if they can be parallelized in the appropriate way. Most parallelization strategies are unexplored, and the relative performance of different methods is unknown. More broadly, *hardware/software* approaches to scalable Bayesian computing, where speedup is obtained through hardware acceleration and high-performance code, rather than novel mathematical theory, are not well-studied. We believe that our work in this paper makes the case that fast generic methods for large classes of problems are possible, and that GPU-accelerated Bayesian computation is worth substantial further exploration.

References

- [1] J. H. Albert and S. Chib. Bayesian analysis of binary and polychotomous response data. *Journal of the American Statistical Association*, 88(422):669–679, 1993 (cit. on pp. 5, 6).
- [2] A. L. Beam, S. K. Ghosh, and J. Doyle. Fast Hamiltonian Monte Carlo using GPU computing. *Journal of Computational and Graphical Statistics*, 2015 (cit. on p. 2).
- [3] L. Breyer, G. O. Roberts, and J. S. Rosenthal. A note on geometric ergodicity and floating-point roundoff error. *Statistics and Probability Letters*, 53(2):123–127, 2001 (cit. on p. 12).
- [4] J. Canny and H. Zhao. Bidmach: Large-scale learning with zero memory allocation. In *NIPS workshop on BigLearning*, 2013 (cit. on pp. 2, 12).
- [5] C. M. Carvalho, N. G. Polson, and J. G. Scott. The horseshoe estimator for sparse signals. *Biometrika*:1–26, 2010 (cit. on p. 5).
- [6] R. Cheng. The generation of Gamma variables with non-integral shape parameter. *Journal of the Royal Statistical Society, Series C (Applied Statistics)*, 26(1):71–75, 1977 (cit. on p. 7).
- [7] N. Chopin and J. Ridgway. Leave Pima Indians alone: binary regression as a benchmark for Bayesian computation. *arXiv:1506.08640*, 2015 (cit. on p. 9).
- [8] B. d. Finetti. La prévision: ses lois logiques, ses sources subjectives. *Annales de l’institut Henri Poincaré*, 7(1):1–68, 1937 (cit. on p. 4).
- [9] S. Geman and D. Geman. Stochastic relaxation, Gibbs distributions, and the Bayesian restoration of images. *IEEE Transactions on Pattern Analysis and Machine Intelligence*, (6):721–741, 1984 (cit. on pp. 1, 4).
- [10] J. Gosling, B. Joy, G. Steele, G. Bracha, and A. Buckley. The Java language specification. 2000. URL: <https://docs.oracle.com/javase/specs/> (cit. on p. 3).
- [11] W. K. Hastings. Monte Carlo sampling methods using Markov chains and their applications. *Biometrika*, 57(1):97–109, 1970 (cit. on p. 1).
- [12] M. Hutter. Jcuda. 2016. URL: <http://jcuda.org> (cit. on p. 3).
- [13] A. Krizhevsky. One weird trick for parallelizing convolutional neural networks. *arXiv:1404.5997*, 2014 (cit. on p. 2).
- [14] J. Langford. Vowpal Wabbit open source project. Tech. rep. Yahoo, 2007 (cit. on p. 12).
- [15] P. L’Ecuyer and R. Simard. TestU01: AC library for empirical testing of random number generators. *ACM Transactions on Mathematical Software*, 33(4):22, 2007 (cit. on p. 8).
- [16] A. Lee, C. Yau, M. B. Giles, A. Doucet, and C. C. Holmes. On the utility of graphics cards to perform massively parallel simulation of advanced Monte Carlo methods. *Journal of computational and graphical statistics*, 19(4):769–789, 2010 (cit. on p. 2).
- [17] E. Makalic and D. F. Schmidt. A simple sampler for the horseshoe estimator. *arXiv:1508.03884*, 2015 (cit. on p. 6).
- [18] M. Manssen, M. Weigel, and A. K. Hartmann. Random number generators for massively parallel simulations on GPU. *The European Physical Journal - Special Topics*, 210(1):53–71, 2012 (cit. on p. 8).
- [19] G. Marsaglia. Xorshift rngs. *Journal of Statistical Software*, 8(14):1–6, 2003 (cit. on p. 8).

- [20] N. Matloff. *Programming on parallel machines*. University of California, Davis, 2011 (cit. on p. 2).
- [21] M. Matsumoto and T. Nishimura. Mersenne Twister: a 623-dimensionally equidistributed uniform pseudo-random number generator. *ACM Transactions on Modeling and Computer Simulation*, 8(1):3–30, 1998 (cit. on p. 8).
- [22] N. Metropolis, A. W. Rosenbluth, M. N. Rosenbluth, A. H. Teller, and E. Teller. Equation of state calculations by fast computing machines. *The Journal of Chemical Physics*, 21(6):1087–1092, 1953 (cit. on pp. 1, 5).
- [23] G. Mingas and C.-S. Bouganis. Parallel tempering MCMC acceleration using reconfigurable hardware. In, *Reconfigurable Computing: Architectures, Tools and Applications*, pp. 227–238. Springer, 2012 (cit. on pp. 2, 12).
- [24] Mobile 3rd Generation Intel Core Processor Family Datasheet. 2013. URL: <http://ark.intel.com> (cit. on p. 9).
- [25] J. Nickolls, I. Buck, M. Garland, and K. Skadron. Scalable parallel programming with CUDA. *ACM Queue*, 6(2):40–53, 2008 (cit. on p. 3).
- [26] Nvidia. CUDA Toolkit Documentation v7.5. 2015 (cit. on pp. 3, 4).
- [27] Nvidia. Nvidia Tesla Kepler Family Datasheet. 2013. URL: <http://www.nvidia.com/tesla/> (cit. on p. 9).
- [28] M. Odersky, P. Altherr, V. Cremet, B. Emir, S. Micheloud, N. Mihaylov, M. Schinz, E. Stenman, and M. Zenger. The Scala language specification. 2004. URL: <http://www.scala-lang.org/> (cit. on p. 3).
- [29] C. P. Robert. Simulation of truncated normal variables. *Statistics and computing*, 5(2):121–125, 1995 (cit. on p. 7).
- [30] J. K. Salmon, M. A. Moraes, R. O. Dror, and D. E. Shaw. Parallel random numbers: as easy as 1, 2, 3. In *2011 International Conference for High Performance Computing, Networking, Storage and Analysis*, 2011, pp. 1–12 (cit. on p. 8).
- [31] J. Sanders and E. Kandrot. *CUDA by example: an introduction to general-purpose GPU programming*. Addison-Wesley, 2010 (cit. on p. 3).
- [32] D. Seita, H. Chen, and J. Canny. Fast Parallel SAME Gibbs Sampling on General Discrete Bayesian Networks. *arXiv:1511.06416*, 2015 (cit. on p. 2).
- [33] J. E. Stone, D. Gohara, and G. Shi. OpenCL: A parallel programming standard for heterogeneous computing systems. *Computing in Science and Engineering*, 12(1-3):66–73, 2010 (cit. on p. 3).
- [34] M. A. Suchard, Q. Wang, C. Chan, J. Frelinger, A. Cron, and M. West. Understanding GPU programming for statistical computation: Studies in massively parallel massive mixtures. *Journal of Computational and Graphical Statistics*, 19(2):419–438, 2010 (cit. on p. 2).
- [35] A. Terenin, D. Simpson, and D. Draper. Asynchronous Gibbs Sampling. *arXiv:1509.08999*, 2016. URL: <http://arxiv.org/abs/1509.08999> (cit. on p. 12).
- [36] Typesafe Inc. Akka Scala Documentation. 2015. URL: <http://akka.io/> (cit. on p. 12).
- [37] W. N. Venables and B. D. Ripley. *Modern Applied Statistics with*. Springer, 2002 (cit. on p. 8).
- [38] F. Yan, N. Xu, and Y. Qi. Parallel inference for latent Dirichlet allocation on graphics processing units. In *Advances in Neural Information Processing Systems*, 2009, pp. 2134–2142 (cit. on p. 2).

- [39] M. Zaharia, M. Chowdhury, M. J. Franklin, S. Shenker, and I. Stoica. Spark: cluster computing with working sets. In *Proceedings of the 2nd USENIX conference on hot topics in cloud computing*. Vol. 10, 2010, pp. 10–16 (cit. on p. 12).